Inorg. Chem. **2005**, *44*, 4961–4968

Geometry of Simple Molecules. 2. Modeling the Geometry of AX_3E and AX_2E_2 Molecules through the Nonbonded Interaction (NBI) Model

Ronald F. See,* Thomas A. Baker, and Pamela Kahler

Department of Chemistry, Indiana University of Pennsylvania, Indiana, Pennsylvania 15705

Received December 17, 2004

A new conceptual model of molecular geometry is presented, called the nonbonded interaction (NBI) model. This model is applied to the geometries of the AX_3E and AX_2E_2 (A = N, O, P, S, As, Se, or Te; X = H, F, Cl, Br, I, CH_3, tBu, CF_3, SiH_3, $Sn(tBu)_3$, or $SnPh_3$) molecule types. For these molecules, the NBI model can be quantified on the basis of a balance between terminal atom–terminal atom (X–X) interactions and lone pair–terminal atom (E–X) interactions. The empirically observed X–A–X angles range from 91.0° (SeH_2) to 180° ($O(Sn(tBu)_3)_2$), and the NBI model predicts the X–A–X angle with a mean unsigned error of 1.0° using the empirical A–X distance, 1.5° using the LMP2/6-31G** A–X distance, and 1.1° using the MMFF94 A–X distance. This level of precision compares well to the LMP2/6-31G**-predicted X–A–X angles and is significantly better than the MMFF94-predicted X–A–X angles. Terminal groups that are not sufficiently spherical (CF_3, SiH_3, and $SnPh_3$) can still be addressed qualitatively by the NBI model, as can molecules with a mixture of terminal groups. The NBI model is able to explain, often quantitatively, the geometry of all of the molecules studied, without any additional postulates or extensive parametrization.

Introduction

The geometry of simple molecules is essential knowledge to a wide range of chemists, and models to explain molecular geometry are universally taught in introductory college chemistry courses. The usual presentation suggests that these models are, at least qualitatively, predictive and that they provide some physical basis for the observed molecular geometry. It is therefore surprising (at least to nontheoretical chemists) that the actual physical basis of molecular geometry remains uncertain and contentious.[1,2]

The molecules of the types AX_3E and AX_2E_2 provide a demanding test for any model of molecular geometry. Empirically determined structures are available for many molecules in these categories, and observed bond angles range from ~90 to 120° (for AX_3E) or 180° (for AX_2E_2). The optimum performance for a conceptual model of molecular geometry would require an explanation (quantitative, if possible) of the geometry of all of these molecules, including the acute and obtuse extremes, without additional postulates or undue complexity. Ideally, the conceptual model should also provide insight as to the physical basis of observed molecular geometries. There is no shortage of proposed models of molecular geometry. Directed valence (hybridization)[3,4] has often been used to rationalize molecular geometry, but Gilheany and others[5−7] have pointed out that this model suffers from several shortcomings: it is difficult to quantify, it cannot explain "unusual" bond angles without additional (and sometimes contradictory) postulates, and it is physically unrealistic. The VSEPR model[8] has received some theoretical support from Bader's work,[9,10] particularly with X = H, but it also cannot explain the geometry trends in the AX_3E molecules[5] and is difficult to quantify. Perturbation theory[5,11] showed promise in explaining the geometries of NH_3, NF_3, PH_3, and PF_3 but is not able to explain the geometries of a

* Author to whom correspondence should be addressed. E-mail: rfsee@grove.iup.edu.

(1) Pophristic, V.; Goodman, L. *Nature* **2001**, *411*, 565.
(2) Mo, Y.; Wu, W.; Song, L.; Lin, M.; Zhang, Q.; Gao, J. *Angew. Chem., Int. Ed.* **2004**, *43*, 1986.
(3) Pauling, L. *The Nature of the Chemical Bond*; Cornell University Press: Ithaca, NY, 1960.
(4) Landis, C. R. In *Advances in Molecular Structures*; Hargittai, I., Hargittai, M., Eds.; JAI Press: Greenwich, CT, 1996; Vol. 2, pp 129−161.
(5) Gilheany, D. G. *Chem. Rev.* **1994**, *94*, 1339.
(6) Burdett, J. K. *Chemical Bonds: A Dialogue*; Wiley: Chichester, U.K., 1997.
(7) Cooper, D. L.; Cunningham, T. P.; Gerratt, J.; Karadakov, P. B.; Raimondi, M. *J. Am. Chem. Soc.* **1994**, *116*, 4414.
(8) Gillespie, R. J.; Hargittai, I. *The VSEPR Model of Molecular Geometry*; Allyn and Bacon: Boston, MA, 1991.
(9) Bader, R. F. W.; Gillespie, R. J.; MacDougall, P. J. *J. Am. Chem. Soc.* **1988**, *110*, 7329.
(10) Bader, R. F. W. *Atoms in Molecules: A Quantum Theory*; Clarendon Press: Oxford, U.K., 1990.

10.1021/ic048211i CCC: $30.25
Published on Web 06/17/2005

wider range of terminal atoms or groups.[12] The vibronic coupling[13,14] model provides a different and interesting approach to molecular geometry, although it has not been applied to a wide range of ligands. Additionally, this model is substantially more complex than other conceptual models, and so it is not easily applicable on a qualitative level.

An essentially different approach is to focus on the repulsive nonbonding forces between terminal atoms and groups rather than the covalent bonds or bonding molecular orbitals. Such a model was initially developed by Bartell,[15,16] and later Glidwell,[17] and was very successful in explaining the geometric trends in substituted alkenes. One of the great strengths of this approach is that it is easily quantifiable (unlike hybridization and VSEPR) and simple enough to be considered a conceptual model. The ligand close-packing (LCP) model is another conceptual framework that is closely related to Bartell's original work and has been the topic of several recent contributions by Gillespie and others.[18−20] The 2001 paper on molecular geometry from this laboratory[12] successfully explained the geometric trends in the AX_3E (A = N or P; X = H, F, or Cl) molecules, which had long been a severe test of conceptual models.[5] While that work used a technique that may be unique to the aforementioned molecules, the conclusions of that study—that the observed geometry is a balance between the X−X nonbonded repulsions and the E−X nonbonded repulsions—are potentially applicable to any molecule with one or more central-atom lone pairs. This concept of molecular geometry as a balance of repulsive forces can be termed the nonbonded interaction (NBI) model. The NBI model is similar to the LCP model, in that they both focus on the repulsive nonbonding forces between terminal atoms or groups (sometimes called 1,3-interactions) as the primary determinant of molecular geometry. However, there is a key difference between NBI and LCP; LCP treats terminal atoms as hard spheres, with radius changing as a function of the central atom to which it is bound. Conversely, NBI uses what is essentially a "soft sphere" approach, where each terminal atom has a single radius and the interaction between terminal atoms can be quantified by the overlap of these radii (Figure 1). On the basis of ref 12, as well as the work of others,[1−11,13−20] it is possible to list the qualitative "foundations" of the NBI model:

(1) The space requirements of terminal atoms and central atom nonbonding electrons (central atom lone pairs) are the primary force determining geometry about that central atom.

(2) The interactions between terminal atoms (X−X interactions) and between a terminal atom and central atom lone pairs (E−X interactions) are repulsive in nature. The X−X interactions can be quantified through the overlap of the X atom radii ("soft-shell" approach).

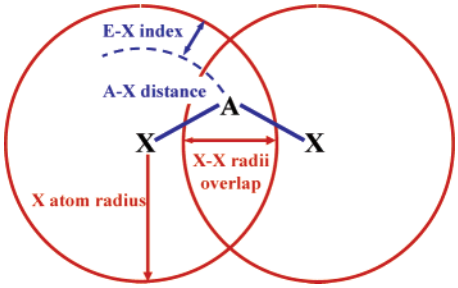

Figure 1. Specified distances in the quantification scheme for the NBI model.

(3) The energy of the electrons associated with a terminal atom is minimized by minimizing the X−X and E−X interactions. These interactions effect the energy of *all* the electrons (A−X bonding electrons, nonbonding electrons on atom X and core electrons) associated with the X atom.

(4) The energy of the central atom lone pair(s) and central atom core orbitals is minimized by minimizing the E−X interactions.

(5) The A−X bond distance is primarily determined by bond order and other attractive electronic effects. However, the magnitude of the X−X and E−X interactions may have a small but significant effect on the A−X distance.

(6) The equilibrium (observed) geometry of the molecule is found in the relative orientation which balances the various repulsive X−X and E−X interactions.

Reference 12 examined a very limited group of molecules and only one molecule type (AX_3E). To provide a more demanding test of the NBI model, a systematic analysis of the AX_3E and AX_2E_2 (where A = N, O, P, S, As, Se, or Te and X = H, F, Cl, Br, I, CH_3, CF_3, SiH_3, *tert*-Butyl, $Sn(tBu)_3$, or $SnPh_3$) molecules was undertaken, using both empirical and computational structural data.

Details of Computations and Data Analysis

Observed and Calculated Equilibrium Structures. The observed structures of the AX_3E and AX_2E_2 molecules were taken from the MOGADOC99 database[21] (for gas electron diffraction and microwave studies) and the Cambridge Structure Database[22] (for X-ray diffraction studies); the data for these empirically observed molecules are collected in Table 1. When multiple structural determinations of the same molecule were available, the structure with the highest precision in bond distances and angles was used.

Calculated structures were computed using the Titan program package.[23] Geometry optimizations were carried out at the 6-31G** level, using HF, B3LYP, and LMP2 computational techniques. All three of these techniques gave results that reproduced the empirical

(11) Cherry, W. R.; Epiotis, N. D.; Borden, W. T. *Acc. Chem. Res.* **1977**, *10*, 167.
(12) See, R. F.; Dutoi, A. D.; McConnell, K. W.; Naylor, R. M. *J. Am. Chem. Soc.* **2001**, *123*, 2839.
(13) Atanasov, M.; Reinen, D. *J. Am. Chem. Soc.* **2002**, *124*, 6693.
(14) Atanasov, M.; Reinen, D. *Inorg. Chem.* **2004**, *43*, 1998.
(15) Bartell, L. S. *J. Chem. Phys.* **1960**, *32*, 827.
(16) Bartell, L. S. *J. Chem. Educ.* **1968**, *45*, 754.
(17) Glidewell, C. *Inorg. Chim. Acta Rev.* **1973**, *7*, 69.
(18) Levy, J. B.; Hargittai, I. *J. Mol. Struct. (THEOCHEM)* **1998**, *454*, 127.
(19) Gillespie, R. J.; Robinson, E. A. In *Advances in Molecular Structures*; Hargittai, I., Hargittai, M., Eds.; JAI Press: Greenwich, CT, 1998; Vol. 4, pp 1−41.
(20) Gillespie, R. J. *Coord. Chem. Rev.* **2000**, *197*, 51.
(21) Vogt, J.; Mez-Starck, B.; Vogt, N.; Hutter, W. *J. Mol. Struct.* **1999**, *485−486*, 249.
(22) (a) Allen, F. H. *Acta Crystallogr.* **2002**, *B58*, 380. (b) Bruno, I. J.; Cole, J. C.; Edgington, P. R.; Kessler, M.; Macrea, C. F.; McCabe, P.; Pearson, J.; Taylor, R. *Acta Crystallogr.* **2002**, *B58*, 389.
(23) *Titan: Tutorial and User's Guide*; Wavefunction, Inc., Schrodinger, Inc.; 1999.

Table 1. Structural Data (Å, deg) for the AX_3E and AX_2E_2 Molecules

	MMFF94		LMP2/6-31G**		empirically determined					
A =	d_{A-X}	X−A−X	d_{A-X}	X−A−X	d_{A-X}	X−A−X	X−X radii overlap	E−X index	type[a]	ref
X = Hydrogen, Radius = 1.28 (Refined)										
N	1.091	106.0	1.013	106.6	1.016	107.5	0.92	0.26	mw	25
O	0.969	104.0	0.962	103.6	0.958	104.5	1.05	0.32	mw	26
P	1.415	94.5	1.405	95.0	1.411	93.4	0.51	−0.13	mw	27
S	1.341	93.4	1.329	92.9	1.336	92.2	0.63	−0.06	mw	26
As	1.537	109.5	1.510	93.0	1.528	91.9	0.36	−0.25	mw	28
Se	1.506	109.5	1.457	91.7	1.459	91	0.48	−0.18	mw	29
X = Fluorine, Radius = 1.47 (Bondi)										
N	1.379	110.4	1.391	102.5	1.365	102.4	0.81	0.11	mw	30
O	1.417	110.4	1.426	102.8	1.409	103.3	0.73	0.06	mw	31
P	1.575	94.8	1.595	98.4	1.563	97.7	0.59	−0.09	mw	32
S	1.591	97.9	1.624	99.1						
As	1.741	109.5	1.710	95.9	1.704	95.8	0.41	−0.23	mw	33
Se	1.762	109.5	1.755	97.5						
X = Chlorine, Radius = 1.75 (Bon di)										
N	1.761	110.4	1.773	107.7	1.754	107.8	0.67	0.00	mw	34
O	1.677	110.4	1.727	110.9	1.700	110.9	0.70	0.05	m/g	35
P	2.100	98.1	2.042	102.5	2.043	100.1	0.37	−0.29	m/g	36
S	2.031	97.9	2.031	103.6	2.010	102.7	0.36	−0.26	mw	37
As	2.171	109.5	2.230	98.9	2.162	98.8	0.22	−0.41	mw	38
Se	2.175	109.5	2.251	99.6	2.157	99.6	0.20	−0.41	ged	39
X = Bromine, Radius = 1.85 (Bondi)										
N	1.857	110.4	2.020	107.6						
O	1.808	110.4	1.923	111.9	1.843	112.2	0.64	0.01	mw	40
P	2.187	98.1	2.280	103.0	2.220	101.0	0.27	−0.37	m/g	41
S	2.156	97.9	2.300	105.4						
As	2.323	109.5	2.520	100.6	2.324	99.9	0.14	−0.47	ged	42
Se	2.321	109.5	2.529	101.4						
X = Iodine, Radius = 1.98 (Bondi)										
N	1.986	110.4	2.196	107.4	2.142	110.0	0.45	−0.16	x	43
O	1.925	110.4	2.041	116.7						
P	2.411	98.1	2.473	104.6						
S	2.341	97.9	2.480	107.3						
As	2.533	109.5	2.738	101.5	2.576	99.2	0.04	−0.60	x	44
Se	2.496	109.5	2.718	103.0						
X = Methyl (CH_3), Radius = 1.60 (Refined)										
N	1.462	110.5	1.460	110.6	1.448	110.6	0.82	0.15	x	45
O	1.421	111.6	1.421	110.0	1.415	111.8	0.86	0.19	m/g	46
P	1.837	100.0	1.846	101.0	1.832	99.2	0.41	−0.23	x	47
S	1.808	98.6	1.806	99.0	1.805	99.1	0.45	−0.21	mw	48
As	1.963	109.6	1.989	96.9	1.964	96	0.28	−0.36	mw	49
Se	1.919	109.6	1.979	96.5	1.945	96.3	0.30	−0.35	mw	50
X = *tert*-Butyl ($C(CH_3)_3$), Radius = 1.87 (Refined)										
N	1.528	118.3	1.534	117.0						
O	1.429	125.9	1.454	126.2	1.436	130.8	1.13	0.43	ged	51
P	1.895	110.9	1.934	107.6	1.911	107.4	0.66	−0.04	x	47
S	1.855	108.8	1.851	112.1	1.854	113.2	0.64	0.02	ged	52
As	2.007	114.4	2.073	105.5						
Se	1.947	116.4	2.035	108.6						
X = Tin Tris(*tert*-butyl ($Sn(tBu)_3$), Radius = 2.72 (Refined)										
O	2.090	135.2	1.931	178.5	1.953	180	1.53	0.77	x	53
S	2.434	124.5	2.460	136.5	2.427	134.2	0.97	0.29	x	54
Se	2.590	126.4	2.652	130.6	2.537	127.4	0.89	0.18	x	54
Te	2.691	129.2	2.868	123.2	2.765	122.3	0.60	−0.04	x	54

[a] Empirical structure types: ged = gas electron diffraction; mw = microwave spectroscopy; m/g = combined ged and mw; x = X-ray diffraction.

molecular structures very accurately (except for when X = Sn(*tert*-butyl)$_3$). The LMP2 technique has the lowest rms error on the X−X distance, and since this distance is the focus of this study, only the 6-31G**/LMP2 structures are detailed in Table 1. However, the nearly equivalent performance of HF, B3LYP, and LMP2 demonstrates that the results of this work are not dependent on the computational technique.

Results and Discussion

E−X Index. In the NBI model, as outlined above, the equilibrium geometry is a function of the competition for space between the various terminal atoms (and/or terminal groups) and central atom lone pairs. While this model can be discussed qualitatively (and will be, below), it is more persuasive to quantitatively demonstrate the ability of the NBI model to explain the geometry of AX_3E and AX_2E_2 molecules. As indicated in ref 12, a simple way to quantify the NBI model in molecules containing at least one central atom lone pair is as a balance between two sets of nonbonded forces (Figure 2). One set of forces result from the repulsions between two X (H or halide) atoms, which are referred to

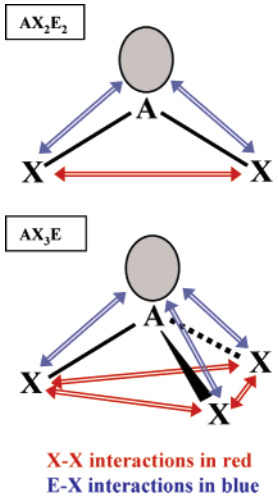

Figure 2. Schematic representation of the quantification scheme for the AX2E2 and AX3E molecules.

as X−X interactions, or 1,3 interactions;[17] these interactions favor a more planar geometry. The other set comprises the repulsions between X atoms and a central atom nonbonding electron pair (lone pair or E), which are referred to as E−X interactions; this set of forces favors more acute X−A−X angles. Each of these sets of nonbonded interactions are highly complex and have an energetic effect on the core orbitals and virtually all the valence molecular orbitals of the molecule. In ref 12, the X−X interactions were quantified by the X−X radii overlap (ro_{xx}; see Figure 1), which is defined as

$$ro_{xx} = (2(radius_x)) - d_{xx} \quad (1)$$

where d_{xx} is the distance between terminal X atoms. Computational data contained in that work indicate that there is a linear relationship between ro_{xx} and the repulsive interaction energy between X atoms, so this quantification technique will be retained. The E−X interactions were formerly quantified by the A−X distance, the rationale being that the distance from the X atom to the centroid of the lone pair (the actual interaction) would be closely related to the A−X bond distance. However, there is a conceptual shortcoming with this approach, namely, that it ignores the different radii of the X atoms. A better approach would be to take the difference between the X atom (or group) radius and the A−X distance; a large positive difference would be indicative of a stronger E−X interaction. This difference will be referred to as the E−X index ($index_{ex}$; see Figure 1) and is defined as

$$index_{ex} = radius_x - d_a \quad (2)$$

where d_{ax} is the A−X distance. Of course, quantifying the E−X interaction in this way assumes that the radial extent of the A atom lone pair is constant. This may not be a completely valid assumption, but reliable values for the radial extent of lone pairs are difficult to determine, so the analysis was made without factoring in this uncertainty. *If it is the case that the observed geometry is at the balance point between the X−X and E−X and interactions, then a plot of ro_{xx} (x-axis) versus $index_{ex}$ (y-axis) should be linear. Furthermore, the equation of the regression line in this plot would serve to quantify the balancing function between the X−X radii overlap and the E−X index.*

Atomic Radii and the Plot of ro_{xx} vs $index_{ex}$. Clearly, the process outlined above requires some set of atomic radii. The van der Waals radii of Bondi[24] were used in ref 12 and gave good results, at least when X was a halide. Using the Bondi values (see Table 1) for $radius_x$, the plot of ro_{xx} versus $index_{ex}$ for the empirically determined structures of AX_3E and AX_2E_2 molecules with A = N, O, P, S, As, and Se and X = F, Cl, Br, and I is given in Figure 3. The data presented in this plot have several significant characteristics. First, the R^2 value of 0.9922 indicates the exceptionally strong fit of these data (which is experimental and, therefore, of limited precision) to the regression line. Second, it is notable that, due to the E−X index, a single line is sufficient for six different central atoms and two different (AX_3E and AX_2E_2) molecule types. Third, many of the E−X index values are negative. This is simply a result of the choice of radii; the smaller the value of the E−X index, the weaker the E−X interaction (so, for instance, $index_{ex} = -0.50$ indicates a weaker interaction than $index_{ex} = -0.30$). Finally, it is worth considering that the van der Waals radii of Bondi were

(24) Bondi, A. *J. Phys. Chem.* **1964**, *68*, 441.
(25) Cohen, E. A.; Pickett, H. M. *J. Mol. Struct.* **1982**, *93*, 83.
(26) Nakata, M.; Kuchitsu, K. *J. Mol. Struct.* **1994**, *320*, 179.
(27) Drean, P,; Paplewski, M.; Demaison, J.; Breidung, J.; Thiel, W.; Beckers, H.; Burger, H. *Inorg. Chem.* **1996**, *35*, 7671.
(28) McRae, G. A.; Gerry, M. C. L.; Wong, M.; Ozier, I.; Cohen, E. A. *J. Mol. Spectrosc.* **1987**, *123*, 321.
(29) Flaud, J.-M.; Camy-Peyret, C.; Arcas, P. *J. Mol. Spectrosc.* **1994**, *167*, 383.
(30) Otake, M.; Matsumura, C.; Morino, Y. *J. Mol. Spectrosc.* **1968**, *28*, 316.
(31) Morino, Y.; Saito, S. *J. Mol. Spectrosc.* **1966**, *19*, 435.
(32) Kawashima, Y.; Cox, A. P. *J. Mol. Spectrosc.* **1966**, *19*, 435.
(33) Smith, J. G. *Mol. Phys.* **1978**, *35*, 461.
(34) Cazzoli, G.; Favero, P. G.; DalBorgo, A. *J. Mol. Spectrosc.* **1974**, *50*, 82.
(35) Nakata, M.; Yamamoto, A.; Fukuyama, T.; Kuchitsu, K. *J. Mol. Struct.* **1983**, *100*, 143.
(36) Kisliuk, P.; Townes, C. W. *J. Chem. Phys.* **1950**, *18*, 1109.
(37) Davis, R. W.; Gerry, M. C. L. *J. Mol. Spectrosc.* **1977**, *65*, 455.
(38) Cazzoli, G.; Forti, P.; Lunelli, B. *J. Mol. Spectrosc.* **1978**, *69*, 71.
(39) Fernholt, L.; Haaland, A.; Seip, R.; Kniep, R.; Korte, L. *Z. Naturforsch. B* **1983**, *38*, 1072.
(40) Mueller, H. S. P.; Miller, C. E.; Cohen, E. A. *Angew. Chem., Int. Ed. Engl*. **1996**, *35*, 2129.
(41) Kuchitsu, K.; Shibata, T.; Yokozeki, A.; Matsumura, C. *Inorg. Chem*. **1971**, *10*, 2584.
(42) Samdal, S.; Barnhart, D. M.; Hedberg, K. *J. Mol. Struct.* **1976**, *35*, 67.
(43) Pritzkow, H. *Z. Anorg. Chim. Acta* **1974**, *409*, 237.
(44) Kniep, R.; Reski, H. D. *Inorg. Chim. Acta* **1982**, *64*, L83.
(45) Boese, R.; Blaser, D.; Antipin, M. Y.; Chaplinski, V.; deMeijere, A. *Chem. Commun.* **1998**, 781.
(46) Beagley, B.; Pritchard, R. G. *J. Mol. Struct.* **1985**, *130*, 55.
(47) Bruckmann, J.; Kruger, C. *Acta Crystallogr.* **1995**, *C51*, 1155.
(48) Demaison, J.; Tan, B. T.; Typke, V.; Rudolph, H. D. *J. Mol. Spectrosc.* **1981**, *86*, 406.
(49) Blom, R.; Haaland, A.; Seip, R. *Acta Chem. Scand. A* **1983**, *37*, 595.
(50) Pandey, G. K.; Dreizler, H. *Z. Naturforsch., A* **1977**, 32, 482.
(51) Liedle, S.; Mack, H.-G.; Oberhammer, H.; Imam, M. R.; Allinger, N. L. *J. Mol. Spectrosc.* **1989**, *198*, 1.
(52) Tsuboyama, A.; Konaka, S.; Kimura, M. *J. Mol. Struct.* **1985**, *127*, 77.
(53) Kerschl, S.; Wrackmeyer, B.; Mannig, D.; Noth, H.; Staudigl, R. *Z. Naturforsch.* **1987**, *42B*, 387.
(54) Batchelor, R. J.; Einstein, F. W. B.; Jones, C. H. W.; Sharma, R. D. *Inorg. Chem.* **1988**, *27*, 4636.

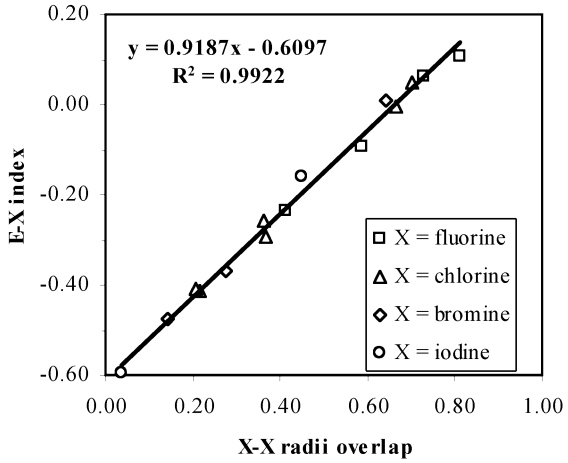

Figure 3. Plot of X−X radii overlap versus E−X index for the AX_3E and AX_2E_2 molecules with X = F, Cl, Br, or I.

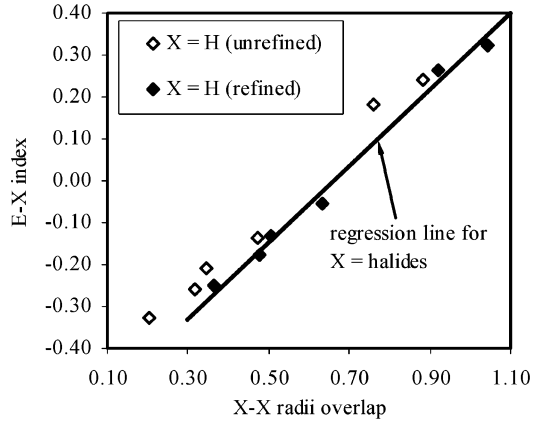

Figure 4. X−X radii overlap versus E−X index for X = H, using the unrefined (1.20 Å) and refined (1.28 Å) $radius_H$ values.

determined from distances *between* molecules and so have little or nothing to do with covalent bonding. The fact that these radius values can be used to explain the geometry *inside* a molecule certainly suggests that nonbonding interatomic interactions have a strong influence on molecular geometry.

When the molecules with X = H, using the accepted van der Waals radius of 1.20 Å, are included in the plot in Figure 3, these points do not fit the regression line (this was also observed in ref 12),[55] although they do appear to be "systematically" in error (see Figure 4). This suggests that the radius value for hydrogen is not consistent with those of the halides, at least for the purposes of this model. The practical solution is to refine the radius value for hydrogen to obtain maximal fit with the regression line from the X = halide molecules; this is found at a $radius_H$ = 1.28 Å, as shown in Figure 4. Similarly, it should be possible to use this refinement technique to determine radius values for some terminal groups, particularly if they are approximately spherical. The terminal groups methyl (Me or CH_3), *tert*-butyl (tBu or $C(CH_3)_3$), and tin tris(*tert*-butyl) ($Sn(tBu)_3$) all gave excellent agreement with the X = halide regression

(55) If one returns to Bondi's work, this is perhaps not surprising. Bondi tabulated three methods of determing the van der Waals radius (the "mean van der Waals radius" is used in this work), and all these methods agree quite closely for the halides. However, for hydrogen, these three values varied by 0.61 Å.

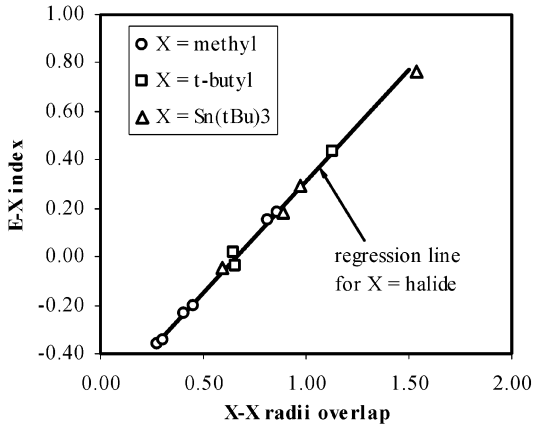

Figure 5. X−X radii overlap versus E−X index for the quasi-spherical terminal groups.

line, as seen in Figure 5, using a single, refined radius value (Me = 1.60 Å, tBu = 1.87 Å, $Sn(tBu)_3$ = 2.89 Å) for each group. For these groups, d_{xx} was defined as the distance between the atoms directly bound to A (i.e., C in CH_3). Some other, less-spherical groups (CF_3, SiH_3, $SnPh_3$) did not give good agreement with the regression line from Figure 3. These groups will not be included in the quantified results, but they will be discussed in qualitative section of this work.

Predicting the X−A−X Angle. As mentioned above, the regression equation for the plot of ro_{xx} versus $index_{ex}$ (Figure 3) serves to quantify the balance between the forces represented by the X−X radii overlap and the forces represented by the E−X index. The fact that the slope is not unity is not surprising, given that the X−X radii overlap and the E−X index arise form somewhat different physical circumstances. The goal of this work is to demonstrate how well the NBI model explains the geometry of the AX_3E and AX_2E_2 molecules. A very clear way to illustrate this point is to use the regression equation ($index_{ex} = 0.9187(ro_{xx}) - 0.6097$) to model, or predict, the X−A−X angle of these molecules; the only additional information that is required is an A−X distance (d_{ax}). If it is recalled that the E−X index is simply the difference between d_{ax} and $radius_x$, then the model X−X radii overlap (ro_{xx}^o) is

$$ro_{xx}^{\,o} = ((radius_x - d_{ax}) + 0.6097)/0.9187 \qquad (3)$$

The model distance between X atoms (d_{xx}^o) are given by

$$d_{xx}^{\,o} = 2(radius_x) - ro_{xx}^{\,o} \qquad (4)$$

The NBI-modeled X−A−X angle is then given by

$$\phi_{xax}^{\,o} = 2(\arcsin((d_{xx}^{\,o}/2)/d_{ax})) \qquad (5)$$

The d_{ax} values used in this modeling were the empirical distances and the distances predicted by the LMP2/6-31G** and MMFF94 calculations; the results of this modeling are given in Table 2. Table 3 compares the NBI-modeled X−A−X angles calculated with the LMP2/6-31G** and MMFF94 A−X distances with the angles computed using those computational methods. Regardless of the source of the A−X distances, the NBI-modeled X−A−X angles are

Table 2. Predicted X−A−X Angles (deg) Using the NBI Model

A =	empirical X−A−X	modeled X−A−X, using: empirical A−X dist	LMP2 A−X dist	MM A−X dist
		X = Hydrogen		
N	107.5	104.7	104.8	101.6
O	105.4	107.6	107.4	107.0
P	93.4	92.5	92.7	92.4
S	92.2	94.2	94.4	94.1
As	91.9	90.3	90.7	90.1
Se	91.0	91.6	91.6	90.7
mean unsigned error		1.8	1.7	2.2
		X = Fluorine		
N	102.4	104.7	103.9	104.3
O	103.3	103.3	102.8	103.0
P	97.7	99.0	98.3	98.7
As	95.8	95.9	95.8	95.2
mean unsign ed error		0.9	0.6	0.9
		X = Chlorine		
N	107.8	108.1	107.6	107.9
O	110.9	109.8	109.0	110.6
P	100.1	101.1	101.1	100.0
S	102.7	101.8	101.3	101.3
As	98.8	98.9	97.7	98.7
Se	99.6	99.0	97.4	98.6
mean unsigned error		0.7	1.3	0.5
		X = Bromine		
O	112.2	110.5	108.2	111.6
P	101.0	101.5	100.4	102.2
As	99.9	99.7	96.7	99.7
mean unsigned error		0.8	2.6	0.6
		X = Iodine		
N	110.0	108.3	107.0	112.5
As	99.2	99.9	97.6	100.6
mean unsigned error		1.2	2.3	2.0
		X = Methyl (CH_3)		
N	110.7	109.9	109.5	109.4
O	111.8	111.2	111.0	111.0
P	99.2	99.1	98.8	99.0
S	99.1	99.7	99.7	99.6
As	96.0	96.6	96.2	96.6
Se	96.3	96.9	96.3	97.4
mean unsigned error		0.5	0.5	0.8
		X = *tert*-Butyl ($C(CH_3)_3$)		
O	130.8	130.1	128.9	130.6
P	107.4	109.5	108.8	109.9
S	113.2	111.2	111.3	111.1
mean unsigned error		1.6	1.8	1.6
		X = Sn(*tert*-butyl)$_3$		
O	180	180	180	180
S	134.2	133.4	131.9	133.0
Se	127.4	128.9	124.9	127.0
Te	122.3	121.5	118.8	123.7
mean unsigned error		0.8	1.9	0.7
overall mean unsigned error		1.0	1.5	1.1

remarkably accurate, with overall mean unsigned errors of 1.0−1.5° in all cases. This compares very well to the mean unsigned error for the LMP2/6-31G**-calculated structures (1.2°) and is far better than the error for the MMFF94-calculated X−A−X angles (6.8°). Special note should be taken of the NBI-modeled angles for X = H, CH_3, tBu, and $Sn(tBu)_3$. These were *not* part of the data used to establish the regression equation, but the NBI modeling scheme outlined above accurately predicts their X−A−X angles. This is all the more impressive in light of the huge range of X−A−X angles in these compounds, from a low of 91.0° in SeH_2 to a high of 180° in $O(Sn(tBu)_3)_2$ (in effect, extrapolated in both directions from the X = halide data).

Table 3. Comparison of Mean Unsigned Error from the Empirically Observed X−A−X Angles

X =	N_{obs}	LMP2 dists: LMP2 computed	LMP2 dists: NBI modeled	MM dists: MM computed	MM dists: NBI modeled
		All Structures			
single atoms	21	1.0	1.6	6.1	1.2
spherical groups	13	1.4	1.3	8.0	1.0
all	34	1.2	1.5	6.8	1.1
		Limited Data Set			
single atoms	11	0.8	1.4	2.9	1.5
spherical groups	7	1.4	1.2	2.1	1.1
all	18	1.0	1.3	2.6	1.3

Notice that so-called "stereochemically inert" lone pairs, such as in $N(tBu)_3$ and $O(Sn(tBu)_3)_2$, are incorporated (and correctly quantified) in the NBI model without any additional postulates (see explanation below).

In all fairness, it should be noted that MMFF94 is not well parametrized for atoms of periods 3 or 4, such as As, Se, Br, Sn, or I. To focus on those AX_3E and AX_2E_2 molecules of the greatest interest, a limited data set was investigated with A = N, O, P, or S and X = H, F, Cl, CH_3, or tBu (18 empirical structures). In this limited data set, the NBI-modeled angle, using the MMFF94-calculated A−X distances, had a mean unsigned error of 1.3°, still far more accurate in prediction of the empirical X−A−X angle than the MMFF94 methodology (mean unsigned error = 2.6°). It should be remembered that the performance of the NBI model is achieved with *one* regression line, an A−X distance, and *one* radius parameter of each of the terminal atoms/groups studied. Not only is the performance of the molecular mechanics package poorer, even for this limited data set, than the NBI modeling but MMFF94 requires *many more* parameters to predict the X−A−X angle[56] than does the NBI quantification scheme.

"Anomalous" Geometries of AX_3E and AX_2E_2 Molecules. Molecules of the AX_3E and AX_2E_2 types are expected, by directed valence and VSEPR, to have angles of ∼109.5° (although both these models recognize some variation of bond angle in the presence of stereochemical lone pairs, so the observed 107.5° bond angle of NH_3 and 104.5 in H_2O might be considered the norm). Therefore, molecules in which X−A−X is < 100° or > 115° do not conform to expectations and might be considered anomalous. However, the great strength of the NBI model is that (unlike hybridization or traditional VSEPR)[5,20] it explains the observed geometries of *all* of these molecules, without any additional postulates or explanations. Both the smallest observed X−A−X angles (91.9° in AsH_3, 91.0° in SeH_2) to the largest (180° in $O(Sn(tBu)_3)_2$, 130.8° in $O(tBu)_2$) are accommodated in one model, with a single explanation.

The molecules with X−A−X < 100° have longer A−X distances and, thus, reduced X−X interactions. It should be noted that, for every X atom or group, the trend in X−A−X angle for the AX_3E molecules is N > P > As,

(56) It should be noted that that many molecular mechanics packages (such as MMFF94) provide estimations of vibrational frequencies, potential energy surfaces, etc., that have not as yet been incorporated into the NBI model.

and the trend in A−X distance is the reverse, N < P < As. This trend is completely analogous for the AX_2E_2 molecules. The A−X distance has a greater effect on the X−X interactions than on E−X interactions. When one compares any NX_3E molecule with its phosphorus analogue, the longer A−X distances in the phosphorus species reduces the X−X interactions more than the E−X interactions, and the result is that the X atoms or groups move closer together to reestablish the balance between X−X and E−X interactions. The net effect is to reduce the bond angle in the phosphorus species.

In the case of AX_3E molecules with trigonal planar, or near-trigonal planar geometries (X−A−X > 115°), very strong X−X interactions are responsible. Among the empirically determined structures in this study, $N(CF_3)_3$ (C−N−C = 117.9°) and $N(SiH_3)_3$ (Si−N−Si = 120.0°) fall into this category. In each case, these molecules have short A−X distances and large $radius_x$ values, resulting in the strong X−X interactions. There have been many suggestions concerning the spatial disposition of the nitrogen lone pair in AX_3E molecules with X−A−X at or near 120°.[5,13,14,54,57−59] However, the NBI model gives an explanation of the observed trigonal planar geometry of these molecules that is completely straightforward. The very strong X−X interactions overwhelm the E−X interactions and force the nonbonding electrons on nitrogen into an energetically unfavorable spatial arrangement both above and below the plane of the X groups. The model outlined in this work, and the data in ref 12, suggest that the conversion to a "stereochemically inert" lone pair is simply the outcome of strong X−X interactions, where the energetic cost of the nonbonding electrons occupying a spatially discontinuous domain is less than what would be incurred by moving the X groups closer together. The fact that the phosphorus and arsenic analogues of $N(CF_3)_3$ and $N(SiH_3)_3$ have X−A−X angles no larger than 97.2° reinforces this interpretation. The longer P−X and As−X distances (relative to N−X) result in reduced X−X interactions and more acute X−A−X angles.

An identical argument explains the geometries of the AX_2E_2 molecules, but with the geometric limit of AX_2E_2 molecules being linear, rather than trigonal planar, there is considerably more scope for X−A−X angles > 115°. The $A(Sn(tBu)_3)_2$ molecules are particularly illustrative. Due to the very large size (and $radius_x$ value) of the $Sn(tBu)_3$ group, $O(Sn(tBu)_3)_2$ adopts a linear geometry. The nonbonding (lone pair) electron densities on the oxygen atom are forced into a less-desirable (presumably ring-shaped) spatial domain by the need for the very large $Sn(tBu)_3$ groups to get as far apart as possible. $S(Sn(tBu)_3)_2$ has longer A−Sn distances than $O(Sn(tBu)_3)_2$ and so the sulfur analogue has weaker X−X interactions and a more acute Sn−A−Sn angle, but the Sn−S−Sn angle is still much larger (134.2°) than normal for a AX_2E_2 molecule. As the A−Sn distance continues to increase in the Se and Te analogues, the Sn−A−Sn angle continues to decrease, exactly as is predicted by the NBI model.

Qualitative Application of the NBI Model. This simple quantification method presented above gives ample, quantified evidence of the ability of the NBI model to explain the geometries of the AX_3E and AX_2E_2 molecules, but it is limited. The quantification scheme is only valid (a) where X is a terminal atom (H, F, Cl, Br, or I) or a highly spherical terminal group (CH_3, tBu, or $Sn(tBu)_3$), (b) when one or more lone pairs are present on the central atom, and (c) for molecules containing only one X group (homoleptical molecules). However, the concepts of the NBI model can be applied, on a qualitative level, to a wide variety of molecules. The NBI model predicts that when A−X distances are short and the X group is large, an unusually wide X−A−X angle will be observed. Table 4 clearly shows this effect, in that each molecule with A = N or O has an unusually large X−A−X angle. The NBI model also predicts that the X−A−X angle should decrease progressively as the central atom gets larger (and the A−X distance gets longer). Table 4 shows that these expectations are completely confirmed in the empirical structures of the AX_3E and AX_2E_2 molecules with X = CF_3, SiH_3, or $SnPh_3$.

Table 4. Observed X−A−X Angles (deg) for X = CF_3, SiH_3, and $SnPh_3$

compd	X−A−X	type (ref)[a]	compd	X−A−X	type (ref)[a]
		X = CF_3			
$N(CF_3)_3$	117.9	ged (60)	$O(CF_3)_2$	119.1	ged (61)
$P(CF_3)_3$	97.2	ged (57)	$S(CF_3)_2$	97.3	ged (62)
			$Se(CF_3)_2$	95.5	ged (63)
		X = SiH_3			
$N(SiH_3)_3$	120	ged (64)	$O(SiH_3)_2$	144.1	ged (65)
$P(SiH_3)_3$	96.5	ged (66)	$S(SiH_3)_2$	98.4	ged (67)
$As(SiH_3)_3$	91.5	ged (66)	$Se(SiH_3)_2$	96.6	ged (68)
		X = $SnPh_3$			
			$O(SnPh_3)_2$	136.7	x (69)
			$S(SnPh_3)_2$	107.5	x (70)
			$Se(SnPh_3)_2$	104.3	x (71)
			$Te(SnPh_3)_2$	103.7	x (72)

[a] Structure type: ged = gas electron diffraction; x = X-ray diffraction.

Another qualitative application of the NBI model is in "asymmetrical" $AXYE_2$ and AX_2YE molecules. A very clear example of this application is in molecules containing both

(57) Marsden, C. J.; Bartell, L. S. *Inorg. Chem.* **1976**, *15*, 2713.
(58) Whangbo, M.-H.; Stewart, K. R. *Inorg. Chem.* **1982**, *21*, 1720.
(59) Bickelhaupt, F. M.; Ziegler, T.; Schleyer, P.v. R. *Organomet.* **1996**, *15*, 1477.
(60) Burger, H.; Niepel, H.; Oberhammer, H. *J. Mol. Struct.* **1979**, *54*, 159.
(61) Lowrey, A. H.; George, C.; D'Antonio, P.; Karle, J. *J. Mol. Struct.* **1980**, *63*, 243.
(62) Oberhammer, H.; Gombler, W.; Willner, H. *J. Mol. Struct.* **1981**, *70*, 273.
(63) Marsden, C. J.; Sheldrick, G. M. *J. Mol. Struct.* **1971**, *10*, 405.
(64) Beagley, B.; Conrad, A. R. *Trans. Faraday Soc.* **1970**, *66*, 2740.
(65) Almeningen, A.; Bastiansen, O.; Ewing, V.; Hedberg, K.; Traetteberg, M. *Acta Chem. Scand.* **1963**, *17*, 2455.
(66) Beagley, B.; Medwid, A. R. *J. Mol. Struct.* **1977**, *38*, 239.
(67) Almenningen, A.; Hedberg, K.; Seip, H. M. *Acta Chem. Scan.* **1963**, *17*, 2264.
(68) Almenningen, A.; Fernholt, L.; Seip, H. M. *Acta Chem. Scand.* **1968**, *22*, 51.
(69) Glidewell, C.; Liles, D. C. *Acta Crystallogr.* **1978**, *B34*, 1693.
(70) Cox, M. J.; Tiekink, E. R. T. *Z. Kristallogr.* **1997**, *212*, 351.
(71) Krebs, B.; Jacobsen, H.-J. *J. Organomet. Chem.* **1979**, *178*, 301.
(72) Einstein, F. W. B.; Jones, C. H. W.; Jones, T.; Sharma, R. D. *Can. J. Chem.* **1983**, *61*, 2611.

(73) This lengthening of the A−X bonds as the stereochemical effect of the lone pair decreases was also noted, from a somewhat different perspective, by Atanasov and Reinen in ref 14.

Table 5. X−A−X Angles in Molecules with X = Methyl or *tert*-Butyl (Computational LMP2/6-31G** Structures)

	dists (Å)		Angles (deg)		
molecule	A−Me	A−tBu	Me−A−Me	Me-A−tBu	tBu−A−tBu
AX_2E_2 Molecules, A = O or S					
$O(CH_3)_2$	1.421		110.0		
$O(CH_3)(tBu)$	1.426	1.450		117.8	
O(tBu)		1.454			126.2
$S(CH_3)_2$	1.806		99.0		
$S(CH_3)(tBu)$	1.810	1.842		103.7	
$S(tBu)_2$		1.851			112.1
AX_3E Molecules, A = N or P					
$N(CH_3)_3$	1.460		110.6		
$N(CH_3)_2(tBu)$	1.467	1.494	108.4	114.6	
$N(CH_3)(tBu)_2$	1.476	1.513		110.3	122.1
$N(tBu)_3$		1.534			117.0
$P(CH_3)_3$	1.846		101.0		
$P(CH_3)_2(tBu)$	1.855	1.899	99.6	104.1	
$P(CH_3)(tBu)_2$	1.861	1.911		102.0	111.3
$P(tBu)_3$		1.934			107.6

the methyl and *tert*-butyl terminal groups, since the A−X distance is very similar but the *tert*-butyl group is significantly larger than the methyl group; the computational (LMP2/6−31G**) structural data for these molecules is shown in Table 5. The AX_2E_2 molecules are the simpler case, and they clearly follow the concepts of the NBI model. The X−A−X angle in the $A(tBu)_2$ molecules is larger than the $A(CH_3)_2$ analogues, due to the tBu−tBu interactions being greater than the Me−Me interactions. The Me−tBu interactions in the $A(CH_3)(tBu)$ molecules should be intermediate between the Me−Me and tBu−tBu interactions, and as expected, the X−A−X angles in the asymmetric molecules are also intermediate between the $A(tBu)_2$ and $A(CH_3)_2$ molecules. Also, as would be predicted from the discussion above, the A = S molecules are have systematically smaller X−A−X angles than the A = O analogues.

The AX_2YE molecules are more complex that the $AXYE_2$ molecules, but the stepwise replacement of methyl by *tert*-butyl about a nitrogen or phosphorus center provides an excellent and instructive example of the qualitative NBI model. In these asymmetric molecules, one must consider not only the balance between X−X and E−X interactions but also between the various, unequal X−X interactions. The Me−N−Me angle in $N(CH_3)_3$ is 110.6°. When one methyl is replaced by the larger *tert*-butyl group, the Me−tBu interactions are stronger than were the Me−Me interactions in $N(CH_3)_3$. This forces the two remaining methyl groups closer together, so as to increase their interaction and balance the larger Me−tBu repulsive interaction. Therefore, the NBI model predicts the more acute Me−N−Me angle (108.2°) in $N(CH_3)_2(tBu)$. When a second *tert*-butyl group replaces a methyl ($N(CH_3)(tBu)_2$), we introduce very strong tBu−tBu interactions into the system. Since the N−tBu bonds are relatively short, a wide tBu−N−tBu angle (122.1°) is expected. Additionally, the tBu−tBu interactions must be balanced by Me−tBu interactions that are stronger than they were in $N(CH_3)_2(tBu)$. Hence, the Me−N−tBu angle is smaller in $N(CH_3)(tBu)_2$ (110.3°) than it was in $N(CH_3)_2(tBu)$ (114.6°). When the third methyl is replaced by *tert*-butyl, very strong tBu−tBu interactions are all around the nitrogen center. The *tert*-butyl groups are forced closer together than they were in $N(Me)(tBu)_2$, and the tBu−N−tBu angle falls to 117.0°. The A = P molecules show a trend that is identical with the nitrogen-centered molecules. Of course, the PX_3E and PX_2YE molecules have longer A−X distances than their nitrogen analogues, so the X−P−X angles are systematically smaller than the corresponding X−N−X angles.

As might be expected from Bartell's work,[15,16] the effect of these increasing X−X repulsive interactions can also be seen in the A−X distances. Each successive replacement of a methyl by *tert*-butyl increases all the X−X interactions and forces the A−X bond to stretch slightly. For instance, the N−Me distance is 1.460 Å in $N(CH_3)_3$, 1.467 Å in $N(CH_3)_2(tBu)$, and 1.476 Å in $N(CH_3)(tBu)_2$. Similar, systematic bond stretching can be seen in every analogous bond distance in Table 5.[73] Both the bond distances and bond angles of the molecules in Table 5 support the foundations of the NBI model given at the beginning of this work.

Concluding Remarks. These results support the thesis that the observed molecular geometry of the AX_3E and AX_2E_2 molecules (and their asymmetric analogues) is primarily determined by repulsive, nonbonding interactions; this thesis is the basis of the NBI model. The NBI model is able to explain (quantitatively, when X is an atom or nearly spherical group) observed bond angles in the AX_3E and AX_2E_2 molecules, from 90 to 180°, without any additional postulates. At least for this set of molecules, a simple quantification scheme allows the NBI model to predict X−A−X angles with accuracy similar to sophisticated MO calculations and much better than that of established molecular mechanics methodology. While the molecule types included in this study are limited to AX_3E and AX_2E_2, it seems reasonable to suggest that the geometry of other, and perhaps most, molecule types may also be primarily determined by repulsive nonbonded interactions.[74] A more developed quantification scheme will be required to successfully model additional molecule types, but these results assert that the NBI model may be an important addition to the conceptual understanding of molecular geometry.

Acknowledgment. The authors wish to thank the Merck/AAAS Undergraduate Science Research Program, the IUP Proposal Development Incentive Program, and the IUP Senate Fellowship Grant Program for funding various portions of this work.

Supporting Information Available: A plot of X−X radii overlap versus E−X index for X = CF_3, SiH_3, or $SnPh_3$ (PDF). This material is available free of charge via the Internet at http://pubs.acs.org.

IC048211I

(74) It is clear that d^8, square-planar coordination complexes do not follow the NBI model, at least as it is presented in this work. Other "non-VSEPR" molecules, such as BaH_2, *may* be explained by the NBI model, though these systems require further study.